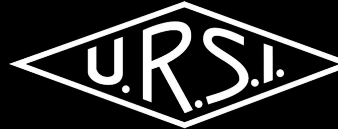




IEEE



E-band feeder link and mechanical phased array antennas for very high-throughput LEO satellite ground terminals

Qi Tang* and B. H. McGuyer

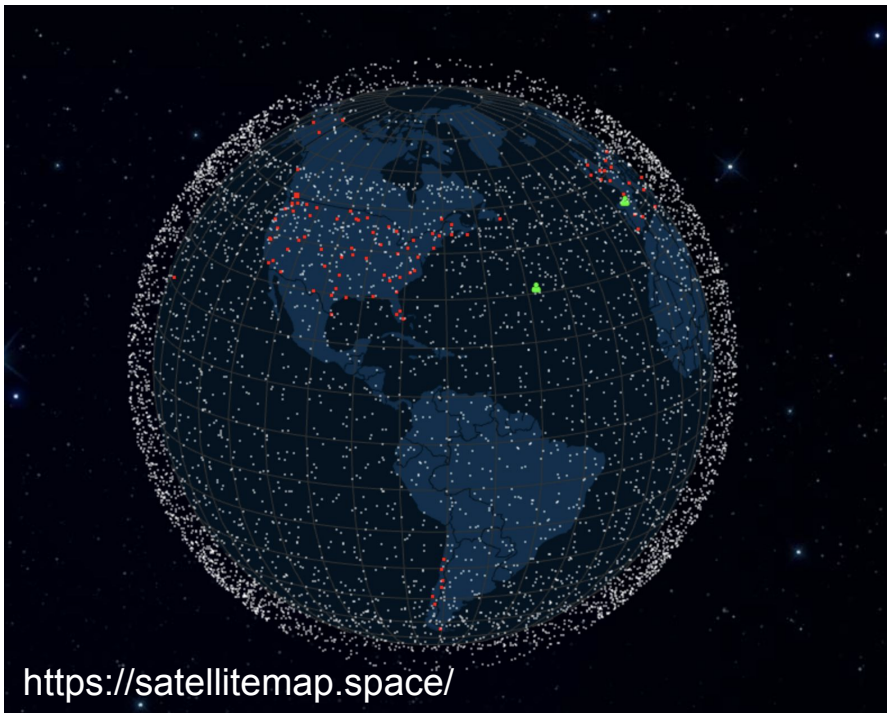
*qitang2023@gmail.com

14 July 2025 • Ottawa, Canada

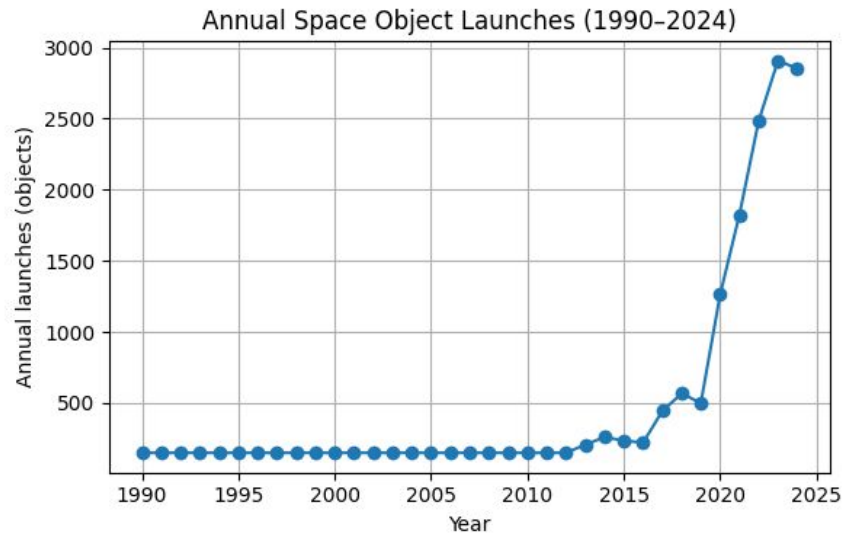
Outlines

- Brief Review on E-band Feeder Links
- Designing and Implementing New Mechanical Steerable Arrays
- Generalized Mechanical Beam-Steering Theory via ***Moiré*** Patterns

Modern Satellite Constellations

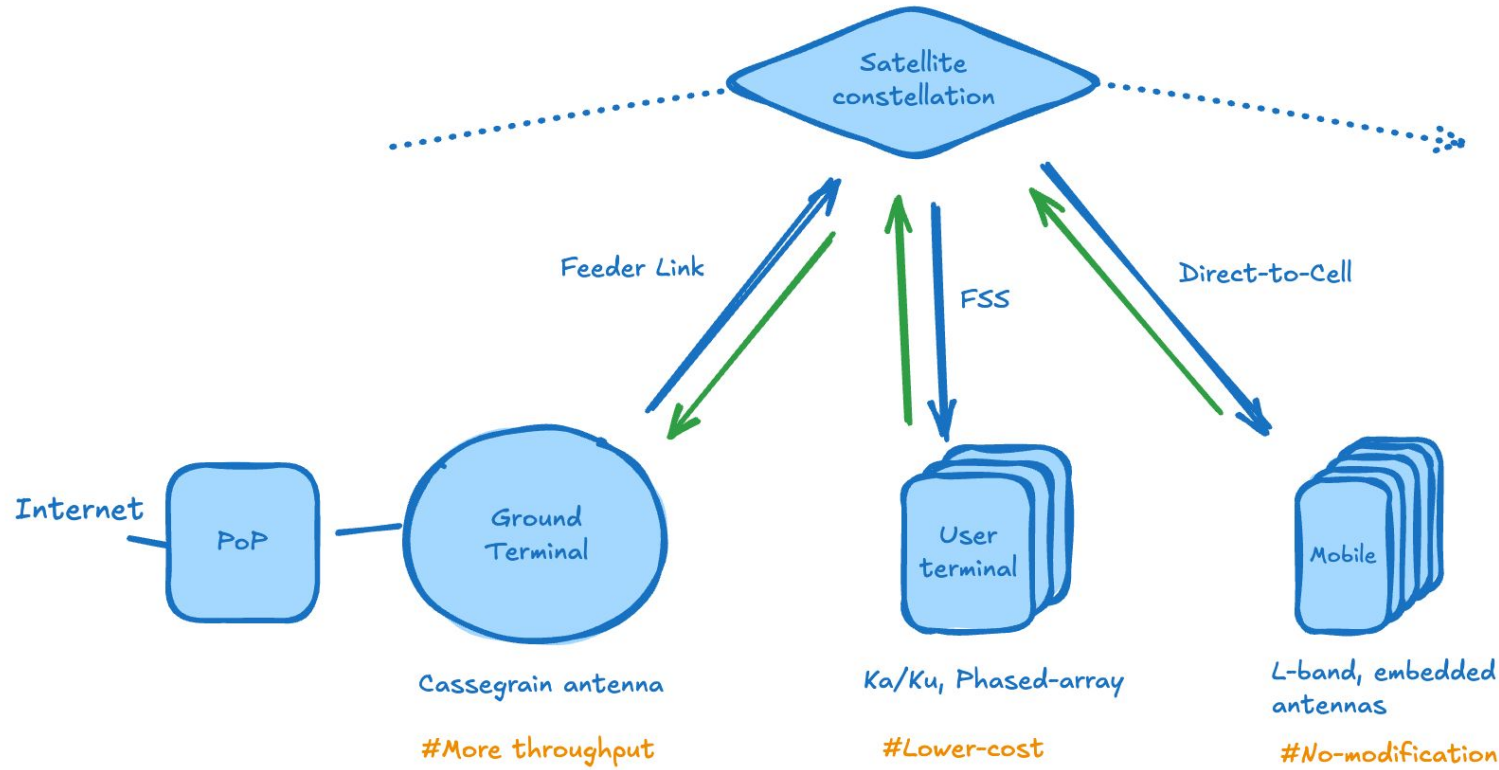


<https://satellitemap.space/>



Constellation	Altitude	Deployed	Planned
Starlink	~550 km	7,875	12,000 (phase 1)
OneWeb	1,200 km	634	882–1,980
Project Kuiper	590 - 630 km	27	3,236

Internet Service (FSS) and Direct-to-Cell



Satellite Communication – Antenna Specs

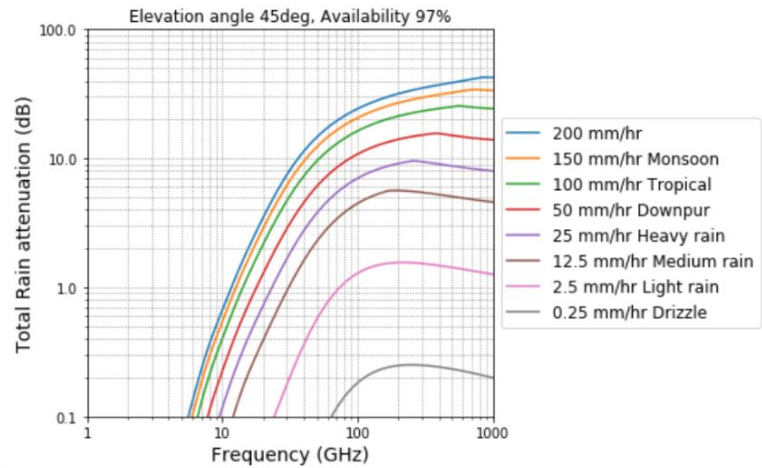
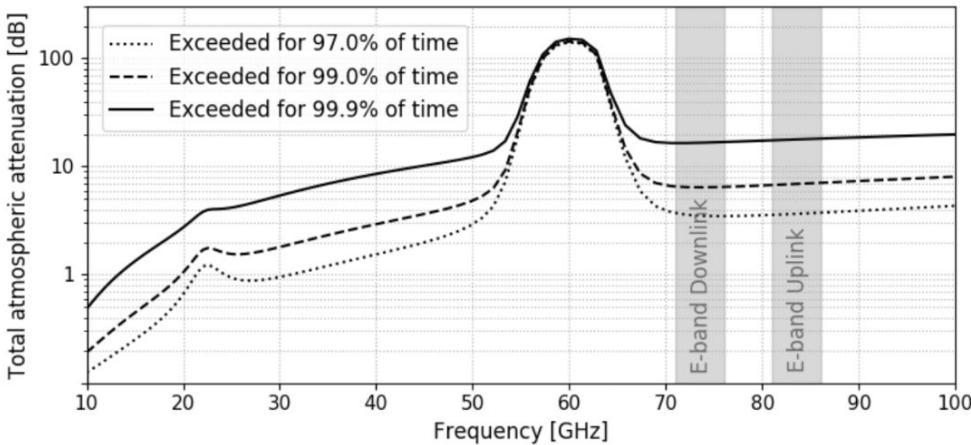
Three types of antennas

1. **Ground terminal** – Cassegrain antennas, high gain and performance, pointing accuracy
2. **User terminal** – low-cost, form-factor (small and flat), beam steering and Beamforming, fast switching / flexibility, ... ⇒ ESA is the proven solution
3. **Mobile device** – omni, on-device, (default built-in top-side mid-band antennas w/o modifications)

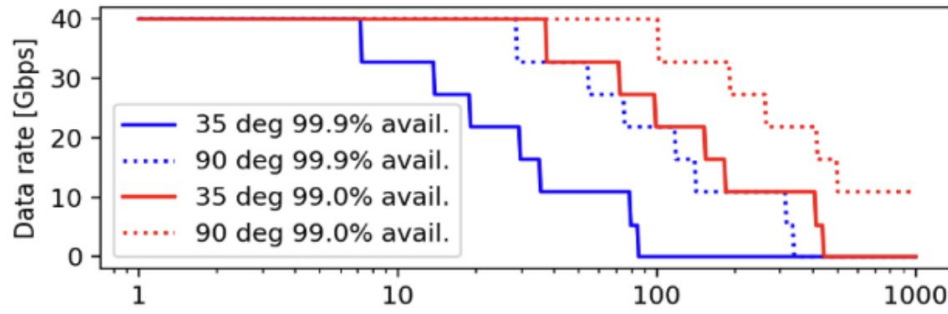
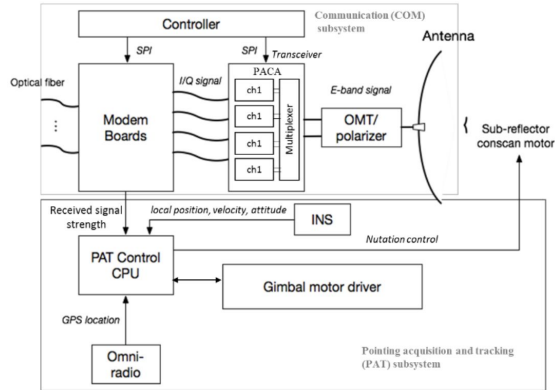
Meet the requirements (by regulatory & carrier's) including EIRP, G/T, beam envelope, XPI, etc.

Advantages of E-band for Non-Terrestrial Links

- Abundant spectrum – 15 GHz total bandwidth
- **Lightly restricted license** – quick, cost-effective but still interference protected
- Robust weather resilience to fog, dust, air turbulence – compared to 60 GHz and laser optics
- Air-to-ground above the weather – **atmospheric and rain loss only exists in the first few km**



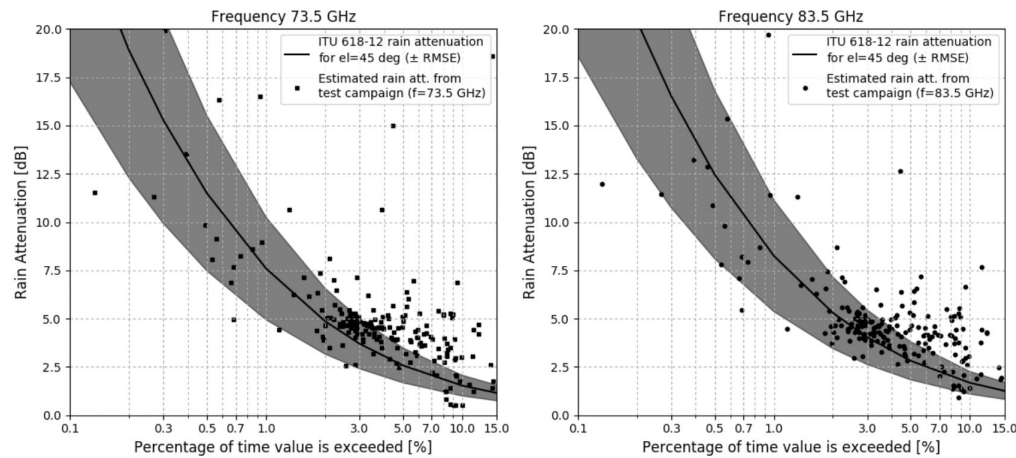
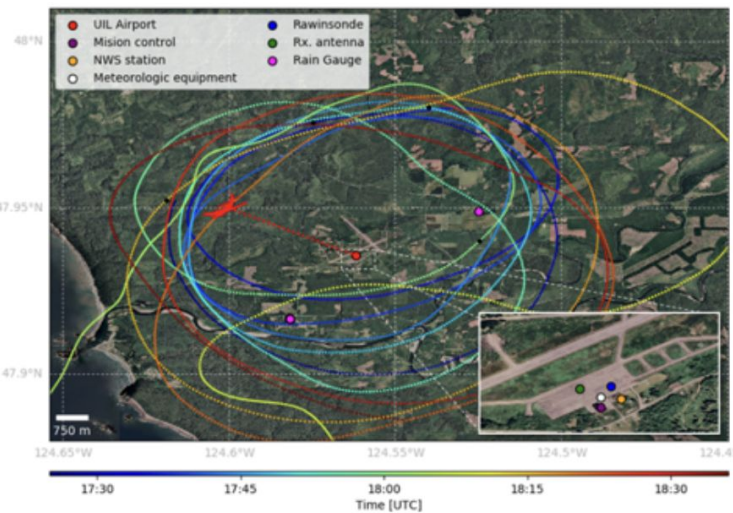
E-band System Design and Prototyping



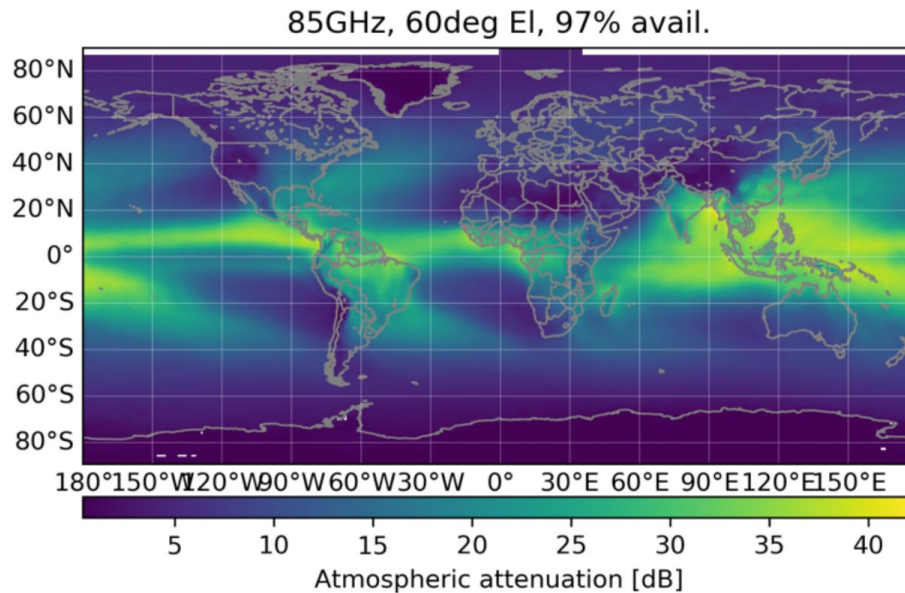
- Demonstrated the first E-band prototype with sustainable **40Gbps air-to-ground** communication system with **COTS parts**
- Airborne terminal consumes 250 Watts power and weighs 11 kg
- Pointing accuracy <0.1° for airborne, <0.02° for ground terminal
- The link sustained up to an altitude of 28 km (99.9% availability in Los Angeles) and **10 Gbps for altitudes over 300 km (with 1.2-meter ground terminal antenna)**

Rain Attenuation Test Campaign

- Test campaign to validate ITU-R P.618-12 estimate on rain attenuation in E-band



Global Total Atmospheric Attenuation Modeling

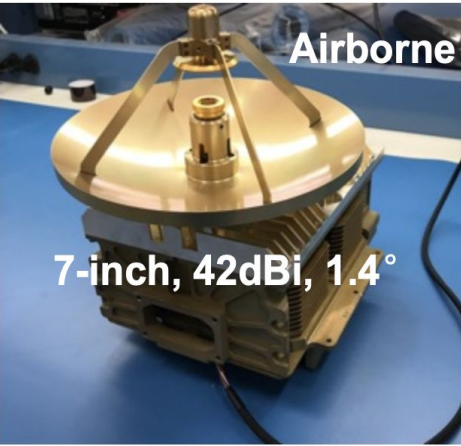


Simple Link Budget Sheet for 64QAM
32Gbps throughput at BER=10⁻⁹

	HAP	LEO satellite
Slant range	50km	1000km
FSPL@85GHz	165	191
Aggr. Ant. Gain	100	100/106
Rx sensitivity	-56	-56
PA power	29	29/40
Margin for Atm. Att. (dB)	20	-6/11

For LEO constellation application, E-band high-throughput link can cover most parts of the world with 80% single terminal link availability and higher link availability (e.g. 99.99%) with multiple (≥ 3) chosen terminal sites

E-band Antennas

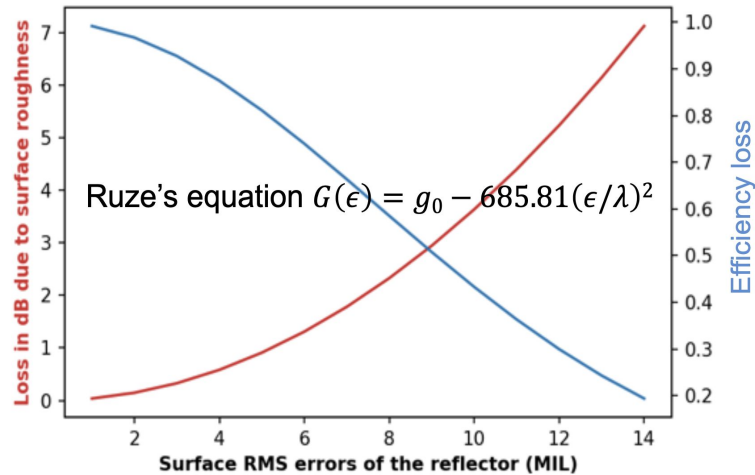


Also in-house implemented 6-ft ~62dBi

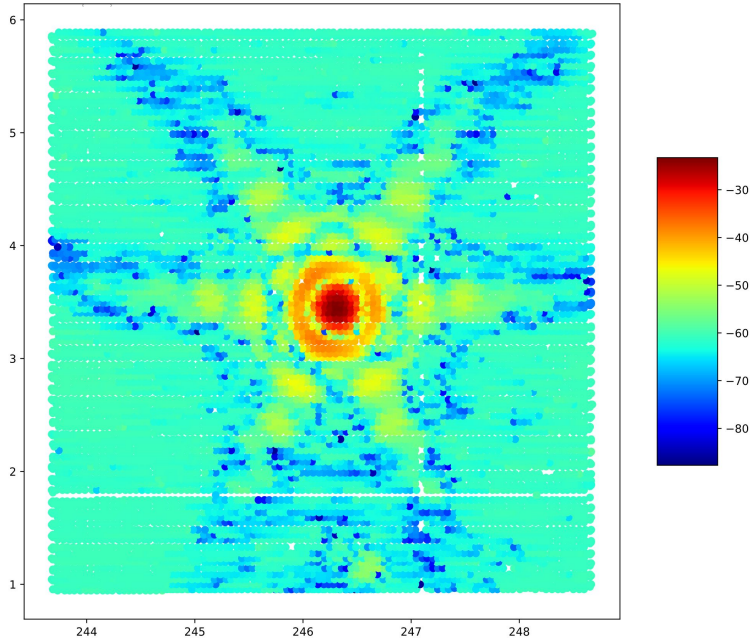
Goal: High gain, pointing accuracy

Surface error (deflection, roughness), weight, wind load, cost

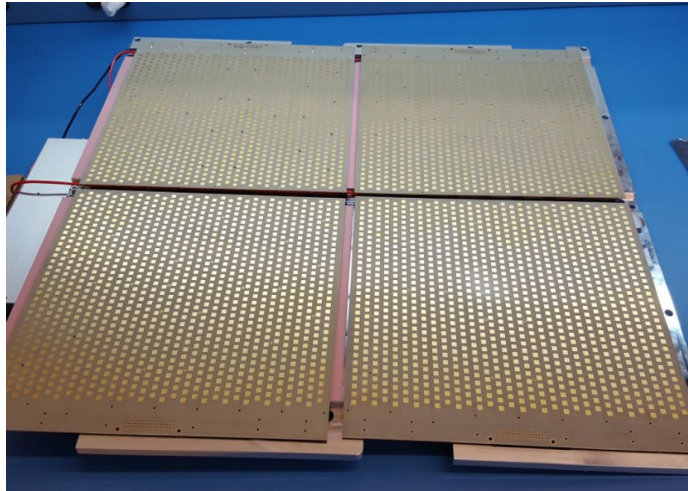
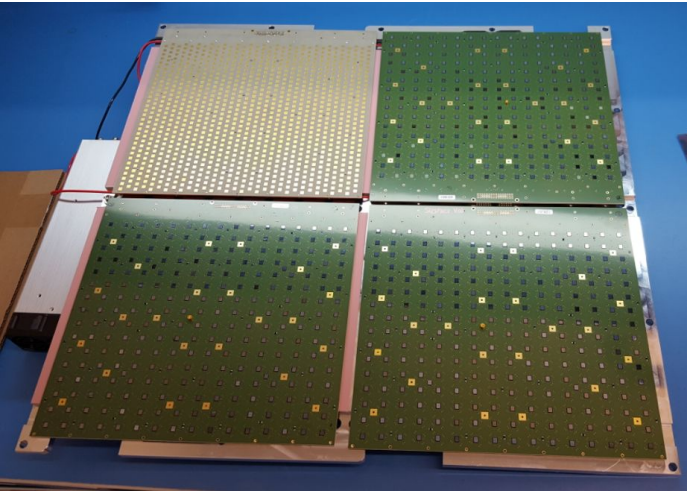
Efficiency loss due to surface roughness



E-band Antenna Measurements



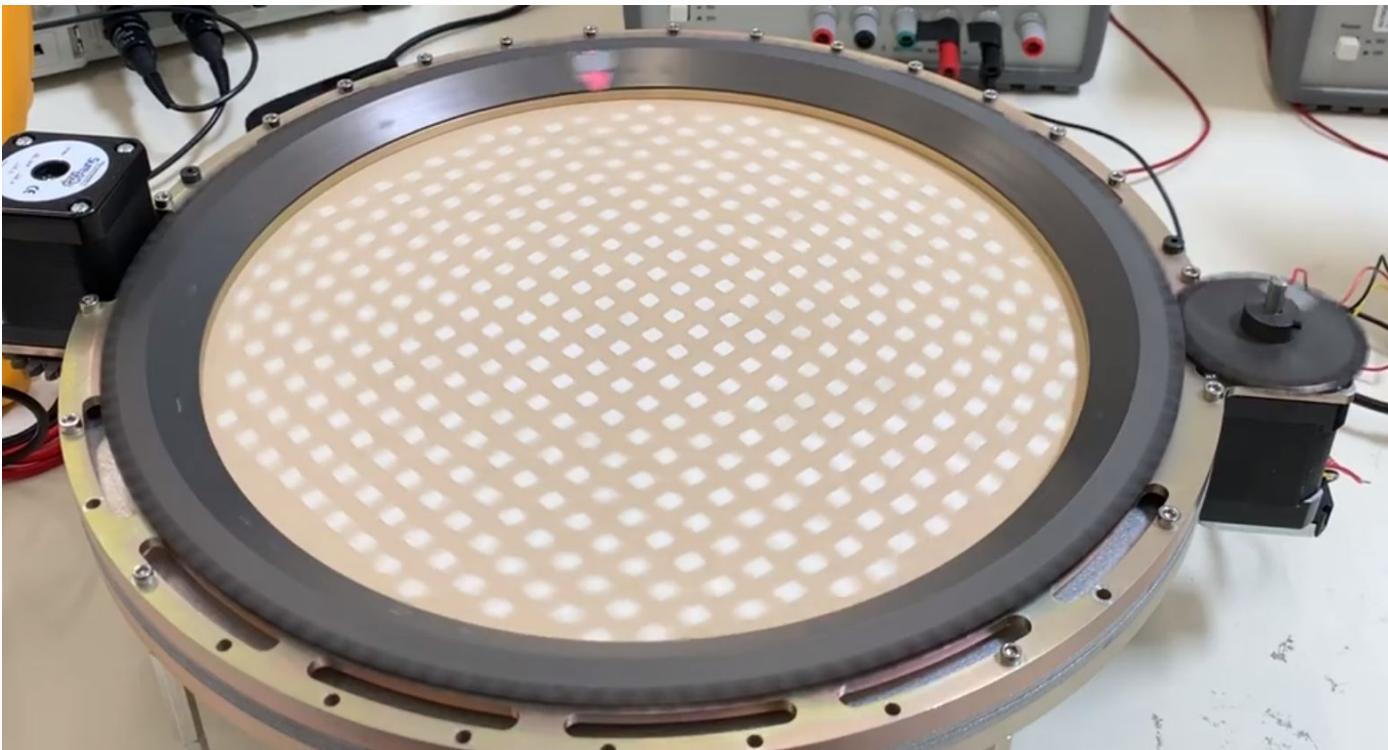
Electronically Steerable Arrays (ESAs)



Designed Ka-band ESA with 4000 elements / 1k chips (by W. Theunissen)

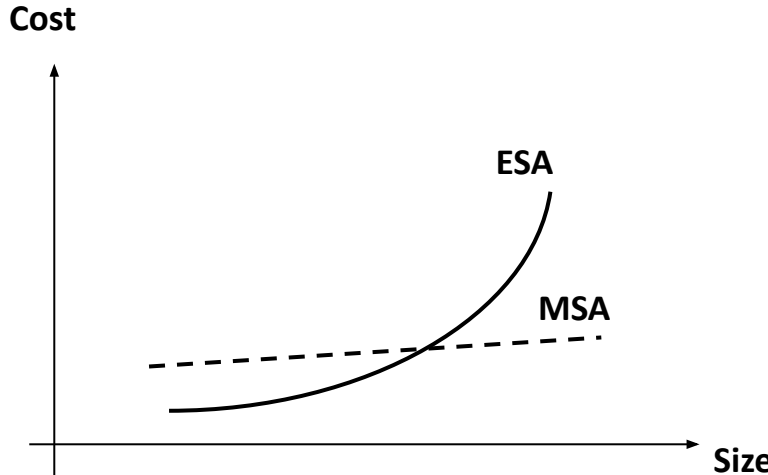
- Electronically steered beams enable rapid scan, multiple beams, and adaptive nulling
- ESAs were VERY costly when firstly built due to the limited chip availabilities.

Mechanical Steerable Array (MSA)

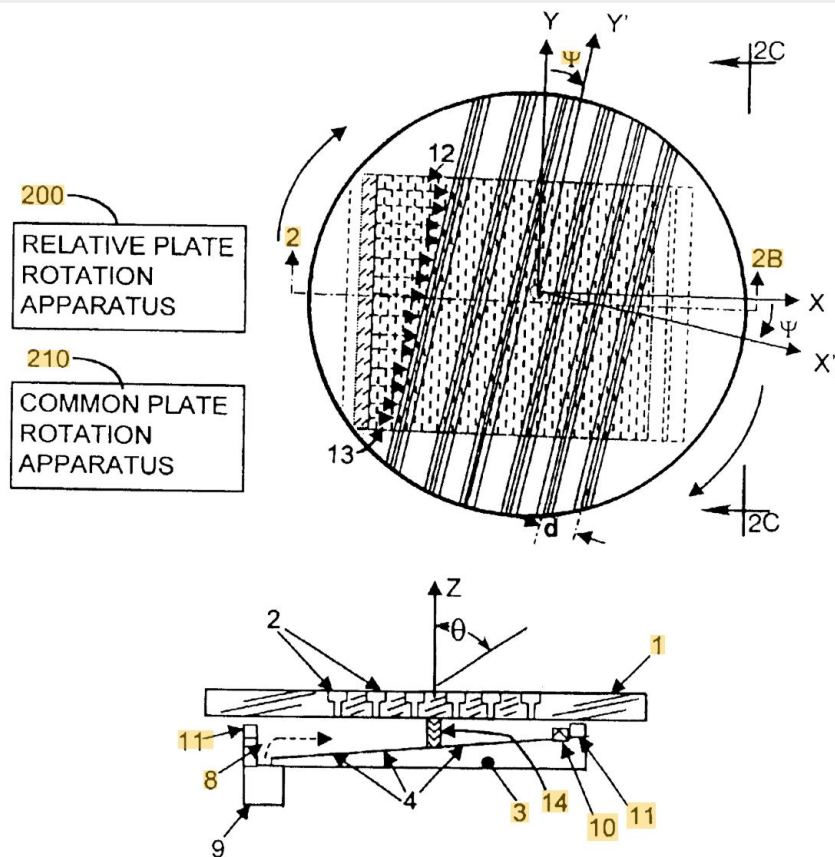


Why MSA?

ESAs use *hundreds or thousands* of chips to steer a beam that ultimately boils down to just control *two* DoFs (θ, φ)



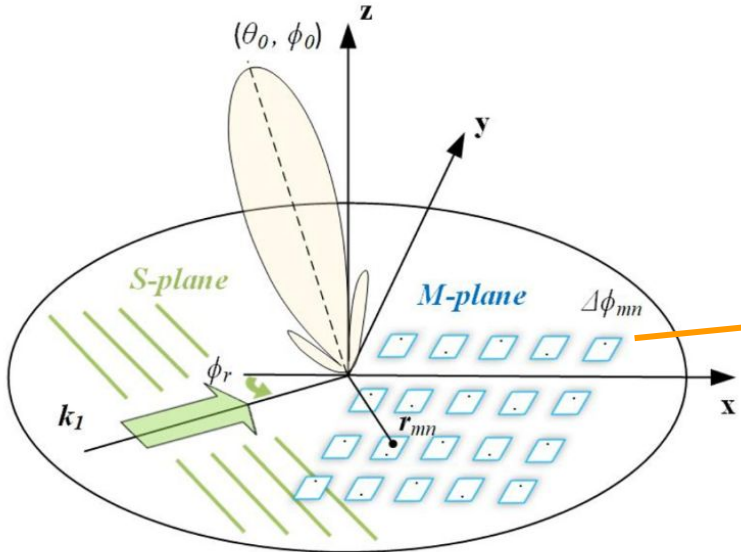
Mechanical Steerable Arrays – VICTS antenna



VICTS – Milroy, W., et al., "Variable inclination continuous transverse stub array," US Patent, 6919854B2, 2005.

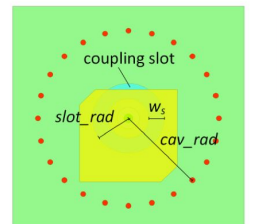
Beam scanning achieved by the in-plane rotation of radiating (Mask-Layer) slots in relative to the quasi-TEM source wave (Source-Layer) in the underlying waveguide

New MSA design

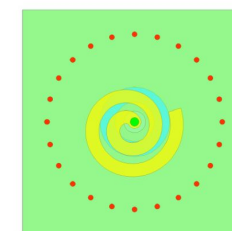


Introduce element-level phase control on the radiating aperture (Mask-plane)

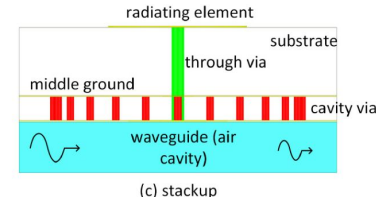
- Simplify the feeding waveguide design (Source-plane) from $k \rightarrow k_0$
- Thus, use parallel plane waveguide instead of complex corrugated / dielectric-filled waveguide



(a) truncated patch

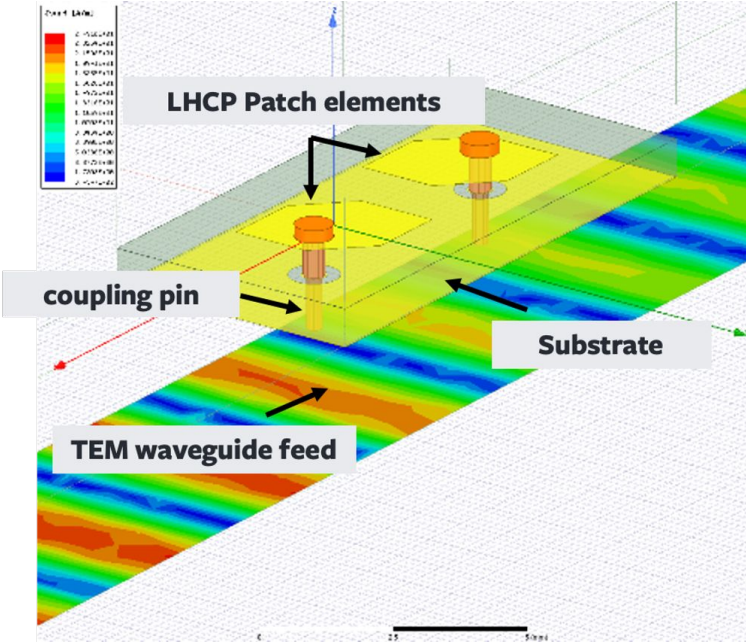


(b) single-arm spiral

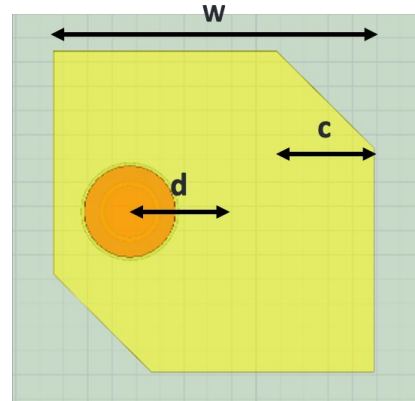


(c) stackup

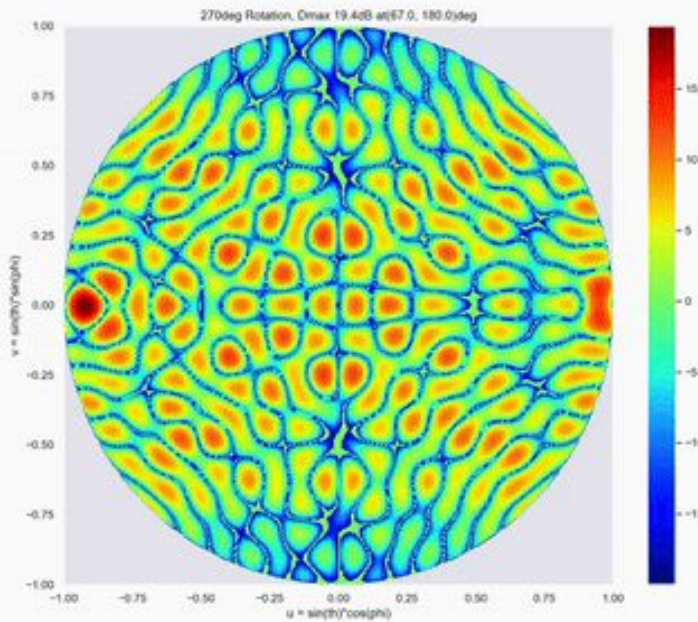
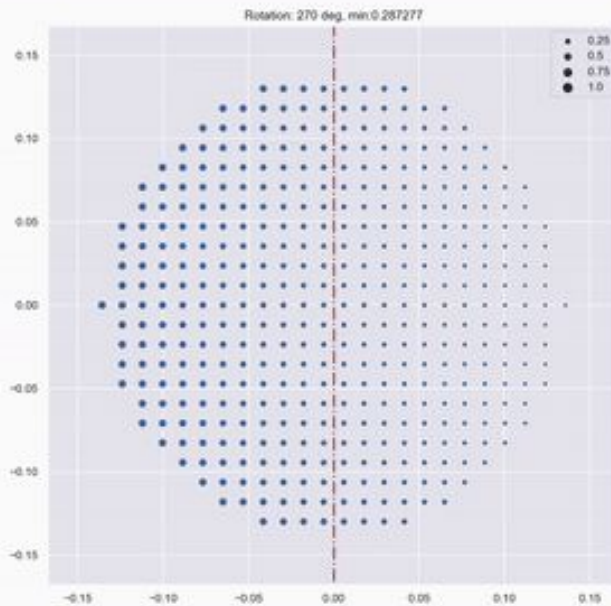
Design Details



Design variables



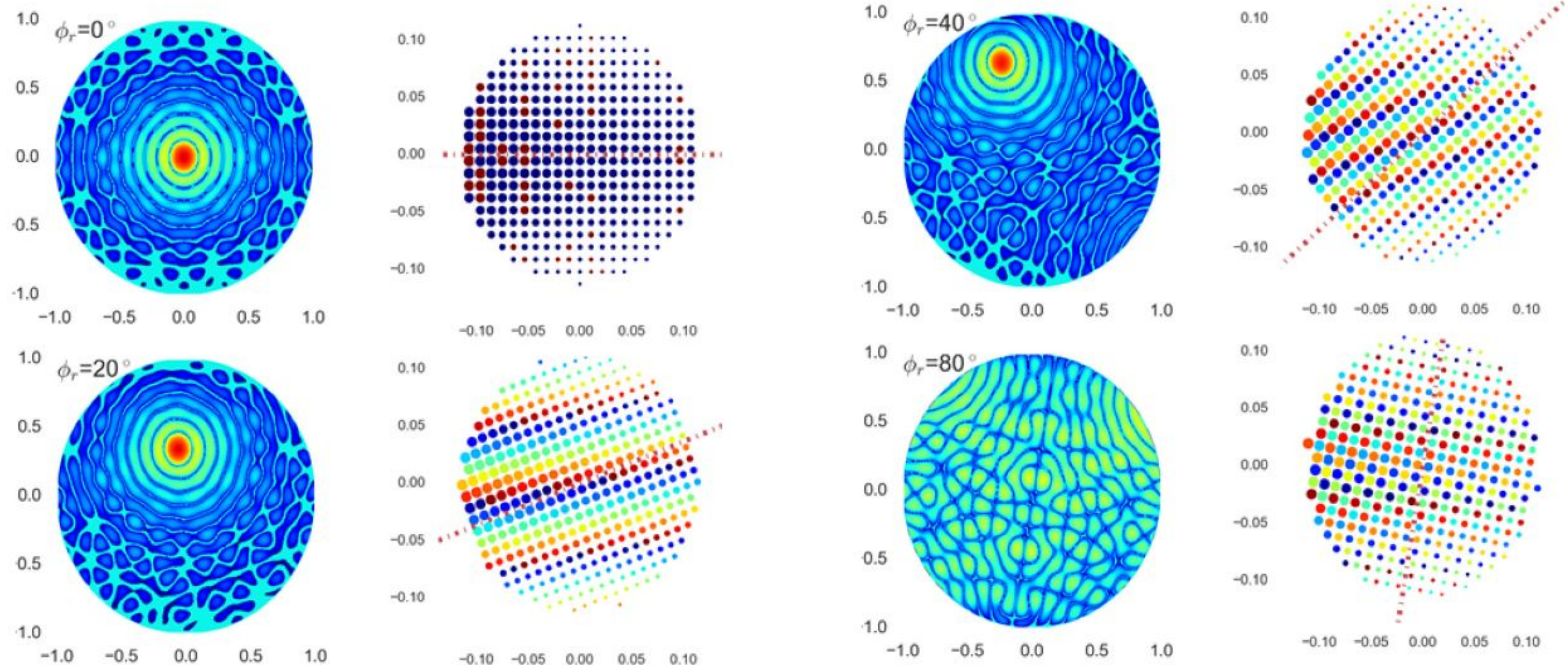
Beam scanning



Simulated radiation patterns (left column) of MSA in 2D polar mapping and the changing phase and amplitude distribution of the element excitations (right column) as the aperture rotates counter-clockwise from 0 to 70.

Radiation Patterns vs. Phase/Amplitude Distributions

Simulated radiation patterns (left column) in 2D polar mapping and the changing phase and amplitude distribution of the element excitations (right column) as the aperture rotates counter-clockwise from 0 to 70.



Mechanical implementations

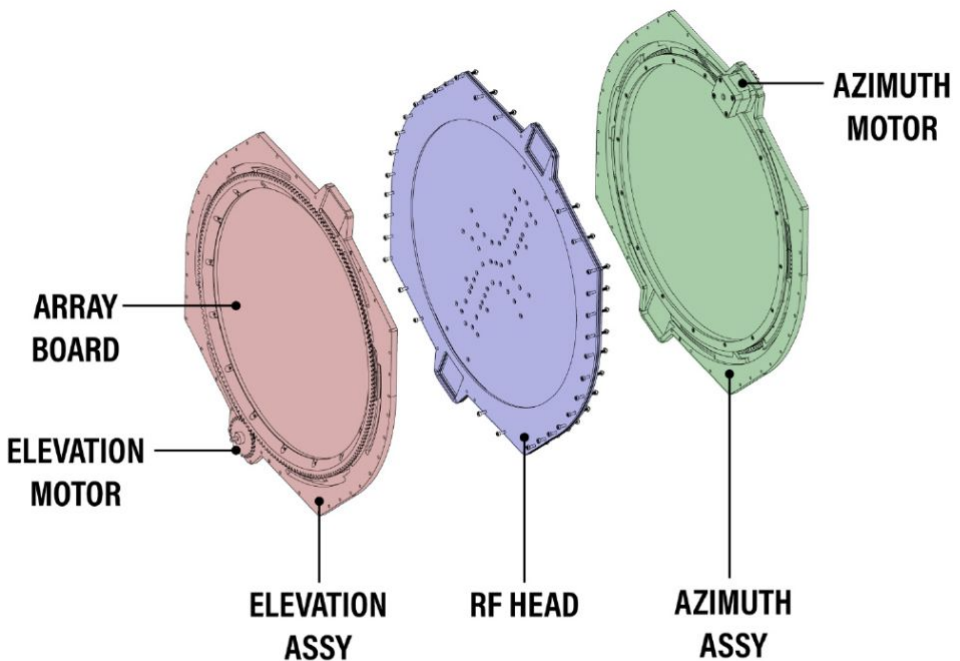
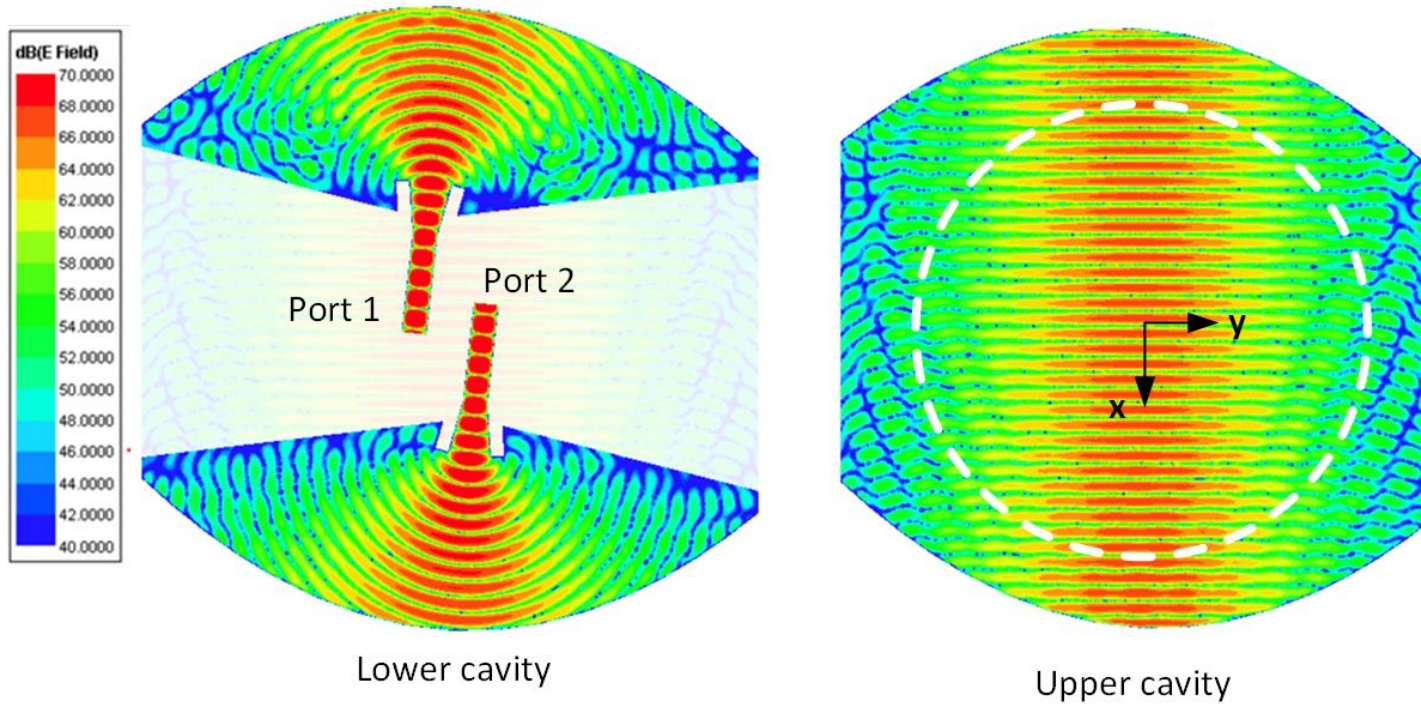


FIGURE 7. Mechanical assembly of the prototype MSAs showing the S-plane (array board), M-plane (RF head), and two motors for full 2D steering.



Waveguide feeds



Radiating elements (Phaser) designs

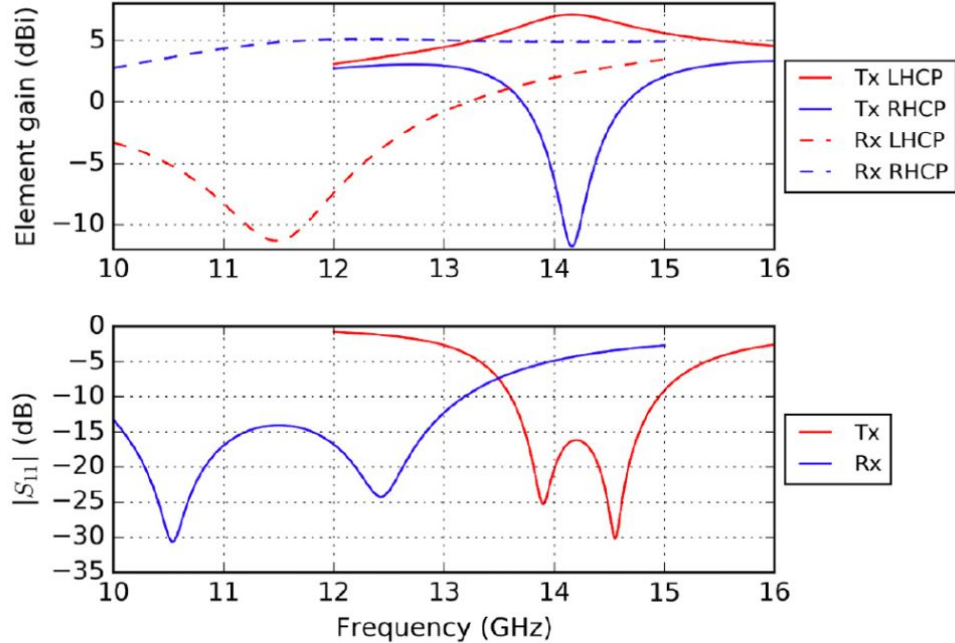


FIGURE 11. (Top) Simulated LHCP and RHC gain of a truncated patch element in the $\phi = 0^\circ$ plane. (Bottom) Input reflection coefficient (S_{11}) as a function of frequency.

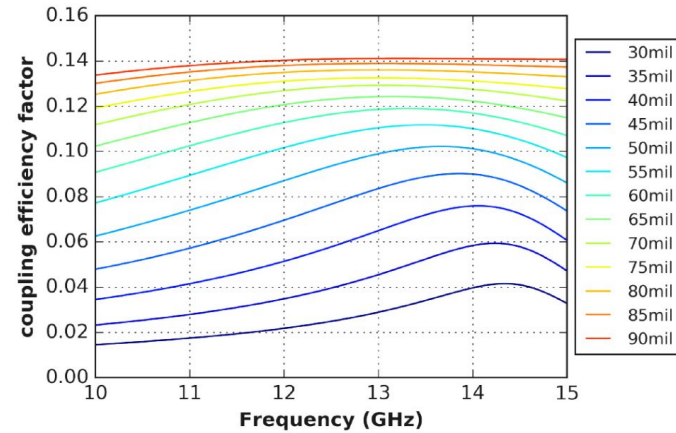
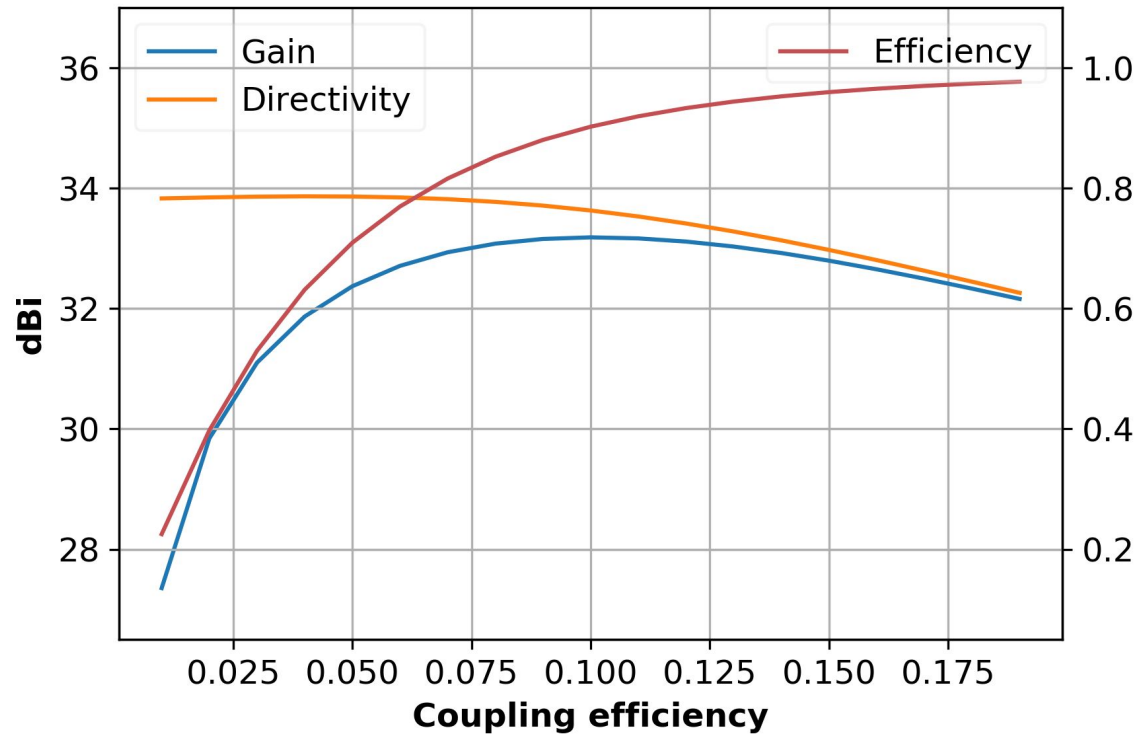
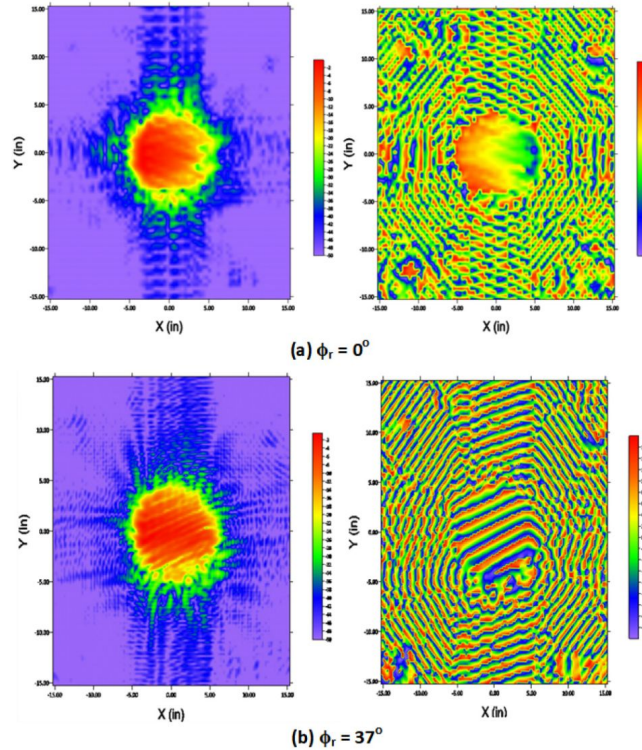
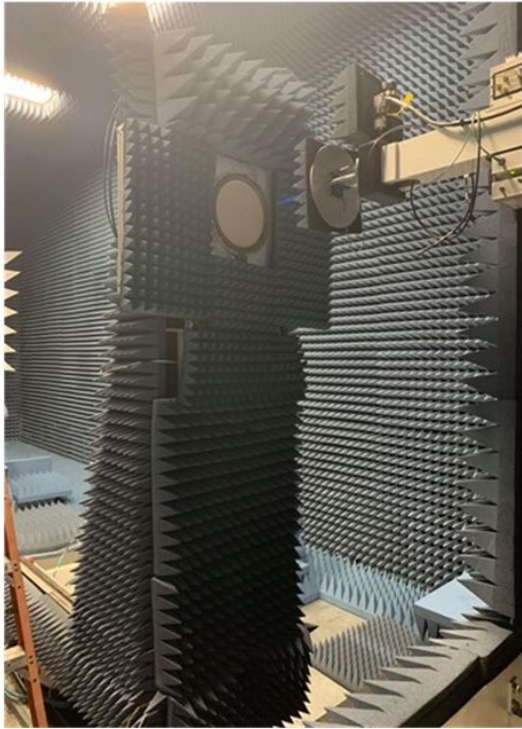


FIGURE 12. Coupling factor curves versus the design parameter $slot_rad$ while $w_s = 15\text{mil}$ and $cav_rad = 170\text{mil}$.

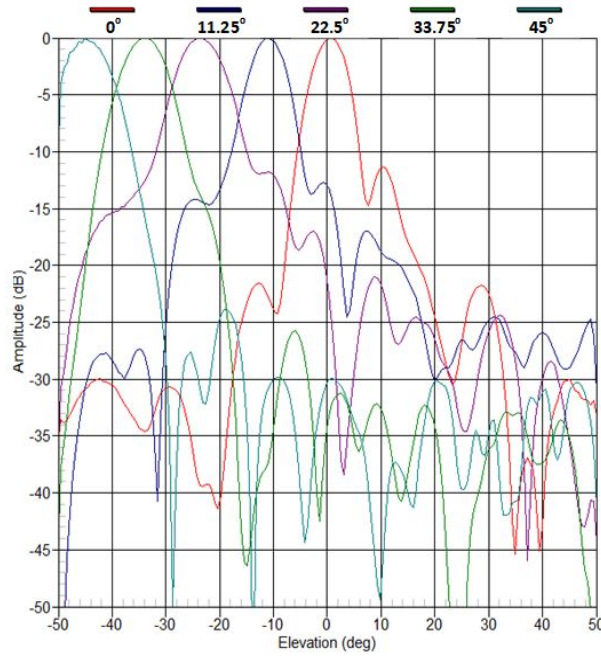
Gain and aperture efficiency



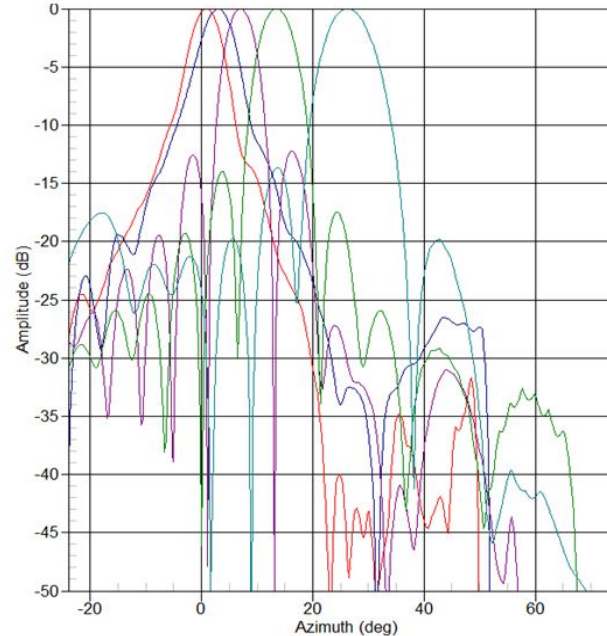
Near Field Scanning on the Aperture Surface



Measured Far-field Radiation Patterns

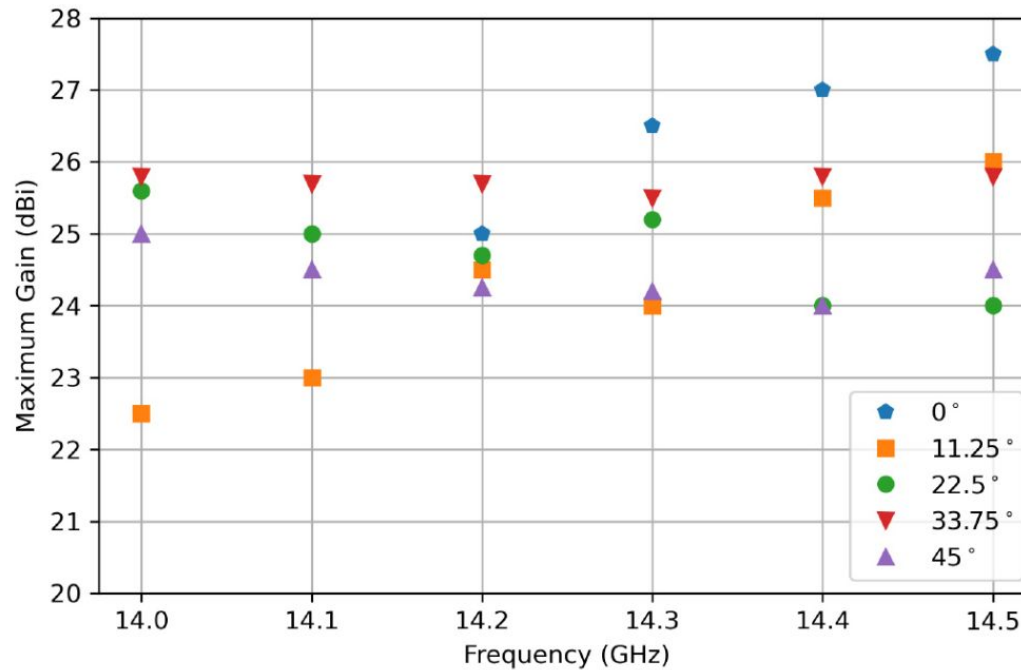


Elevation Angle



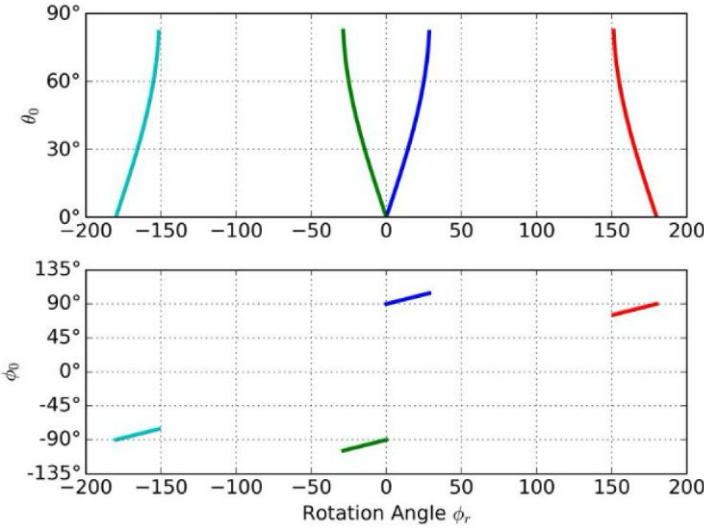
Azimuth Angle

Measured Maximum Gain

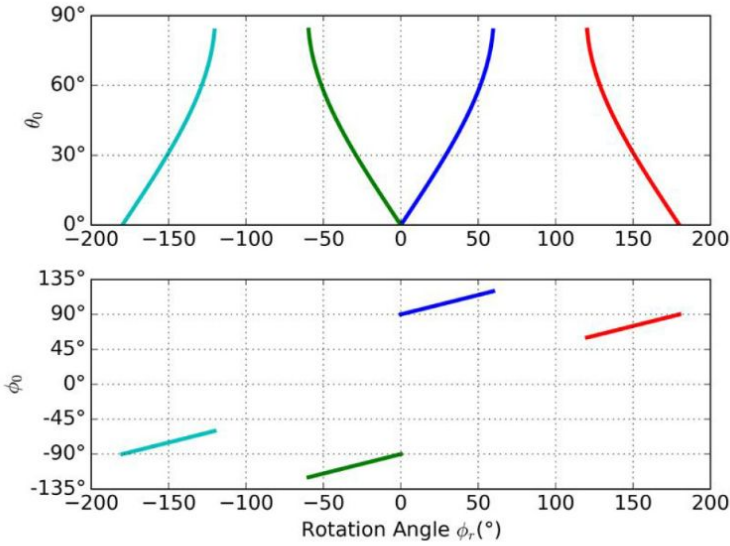


Peak Gain Beam Steering Trajectory – VICTS vs. MSA

VICTS Array



Our MSA design



$$\theta_{pq}(\phi_r) = \arcsin \left[4(1 + p^2) - 8p \cos \phi_r \right]^{1/2}$$

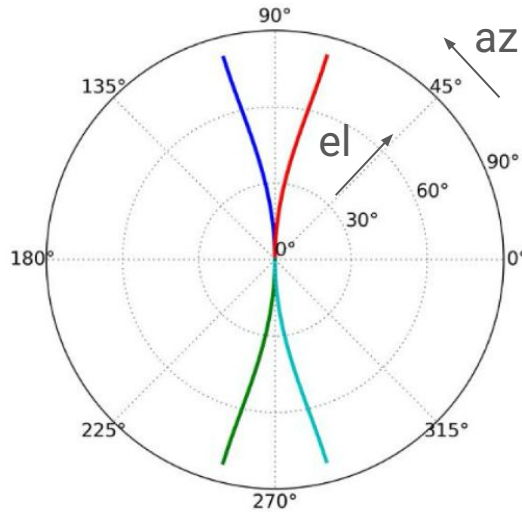
$$\phi_{pq}(\phi_r) = \arctan \left[\frac{\sin \phi_r}{\cos \phi_r - p} \right].$$

$$|\theta_0| = \arcsin |2 \sin(\phi_r/2)| \in [0, \pi/2]$$

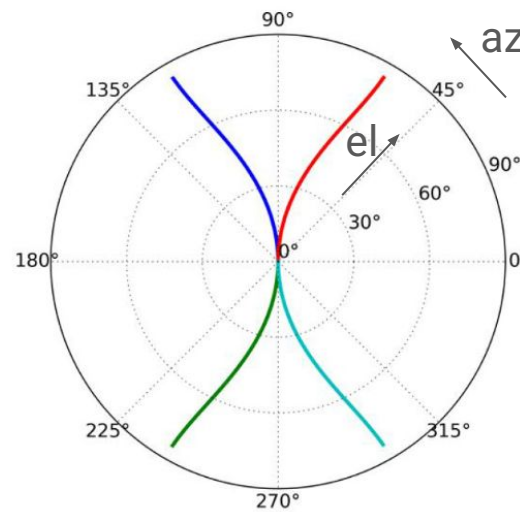
$$\phi_0 = \begin{cases} (\phi_r - \pi)/2, & \phi_r \in (-\pi/3, 0], \\ (\phi_r + \pi)/2, & \phi_r \in [0, \pi/3]. \end{cases}$$

Peak Gain Beam Steering Trajectory – a Top View

VICTS Array



Our MSA design



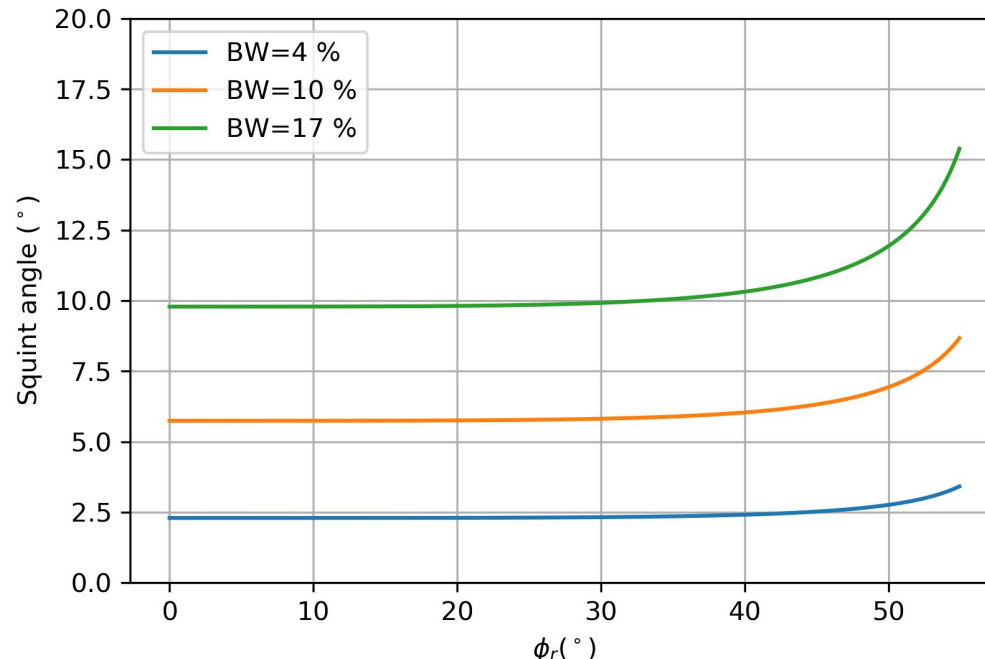
$$\theta_{pq}(\phi_r) = \arcsin \left[4 \left(1 + p^2 \right) - 8p \cos \phi_r \right]^{1/2}$$

$$\phi_{pq}(\phi_r) = \arctan \left[\frac{\sin \phi_r}{\cos \phi_r - p} \right].$$

$$|\theta_0| = \arcsin |2 \sin(\phi_r/2)| \in [0, \pi/2)$$
$$\phi_0 = \begin{cases} (\phi_r - \pi)/2, & \phi_r \in (-\pi/3, 0], \\ (\phi_r + \pi)/2, & \phi_r \in [0, \pi/3). \end{cases}$$

Beam Squint Angle

The maximum squint angle of the beam at different relative bandwidth as different rotations angles.



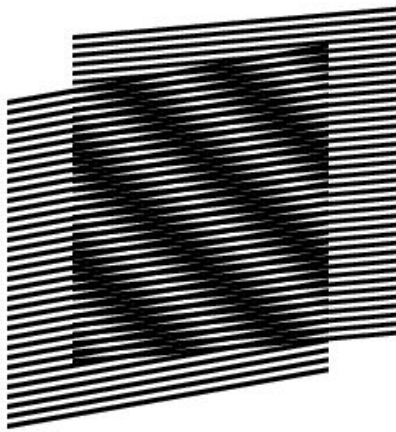
Reflections

What is causing the trajectory difference between MSA and VICTS?

Is there any other mechanical beam-steering schemes besides of rotations?
e.g. **translations, scaling, shearing, twisting**, etc.

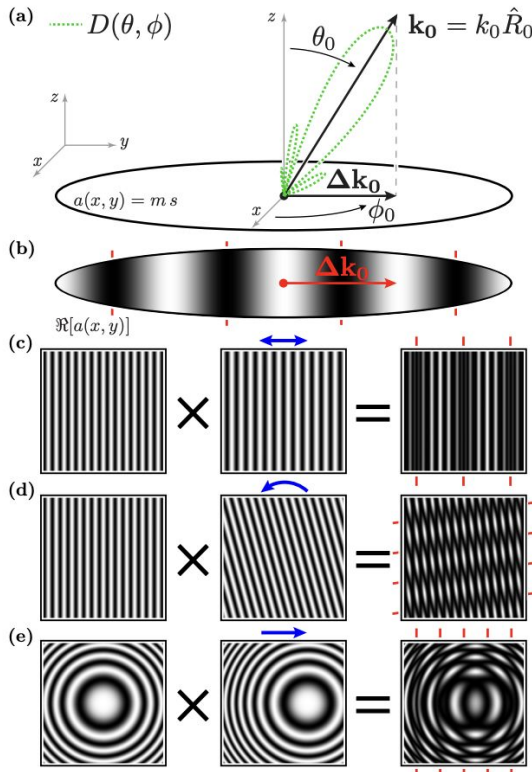
⇒ We need a more generalized theory for mechanical steerable arrays

Moiré Patterns



For more, see *B. H. McGuyer and Q. Tang, "Connection between antennas, beam steering, and the Moiré effect," Phys. Rev. Applied 17, 034008 (2022)*

Connection between Moiré and Antennas



The far-field pattern is a **2D Fourier transform** of its **aperture** distribution

$$D(\theta, \phi) \approx C_0 | K(\theta) \mathcal{F}[a](u(\theta, \phi), v(\theta, \phi))|^2$$

Decompose **aperture** into **source** and **mask** layer

$$a(x, y) = s(x, y)m(x, y)$$

Generate **new steering law**, the phase arguments must

$$g_s(x, y) - g_m(x, y) = u_0 x + v_0 y + w_0 \pmod{2\pi}$$

A generalized mechanical beam-steering principle

1. A mechanically-achievable transform

$$T : (x, y) \mapsto (x', y')$$

you can implement on your mask (rotate, slide, shear, bend, twist...).

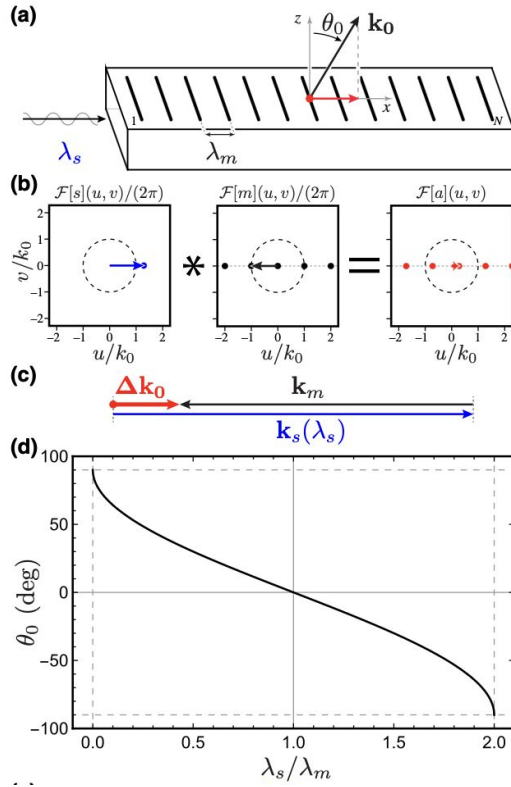
2. A feed-field phase $g_s(x, y)$

one that corresponds to a real electromagnetic excitation at the aperture.

3. The beam steering condition is

$$g_s(x, y) - g_m(T(x, y)) = u_0 x + v_0 y + w_0 \pmod{2\pi}.$$

Scalings



A one-dimensional scaling of the mask by factor α :

$$T_\alpha(x, y) = (\alpha x, y).$$

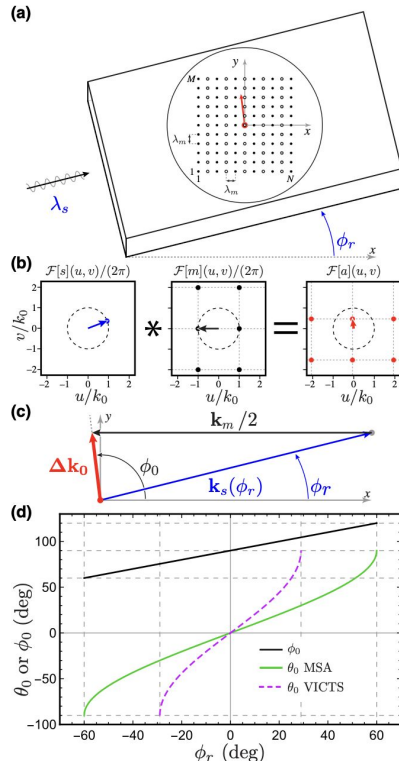
Source and mask phases

$$s_2(x, y) = s_0 e^{i k_s x}, \quad m_2(x, y) \approx m'_0 e^{-i k_m x} w(x).$$

Steering-law substitution

$$g_s(x, y) - g_m(T_\alpha(x, y)) = k_s x - k_m(\alpha x) = (k_s - \alpha k_m) x.$$

Rotations



A rotation of the mask by angle ϕ_r :

$$T_{\phi_r}(x, y) = (\cos \phi_r x + \sin \phi_r y, -\sin \phi_r x + \cos \phi_r y).$$

Source and mask phases (MSAs)

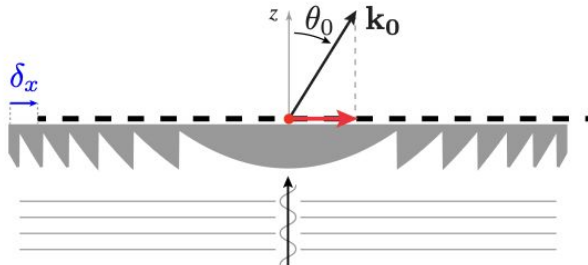
$$s_4(x, y) = s_0 \exp(i k_s [\cos \phi_r x + \sin \phi_r y]), \quad m_4(x, y) \propto e^{-i(k_m/2)x} w(x, y).$$

Steering-law substitution

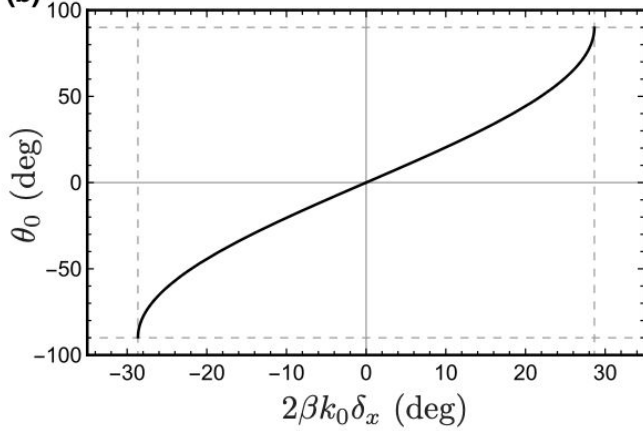
$$\begin{aligned} g_s(x, y) - g_m(T_{\phi_r}(x, y)) &= k_s [\cos \phi_r x + \sin \phi_r y] - \frac{k_m}{2} (\cos \phi_r x + \sin \phi_r y) \\ &= \left(k_s - \frac{k_m}{2} \right) (\cos \phi_r x + \sin \phi_r y) = u_0 x + v_0 y, \end{aligned}$$

Translations (Schuster Fringes)

(a)



(b)



A translation of the mask by (δ_x, δ_y) :

$$T_{(\delta_x, \delta_y)}(x, y) = (x - \delta_x, y - \delta_y).$$

Source and mask phases (Schuster fringes):

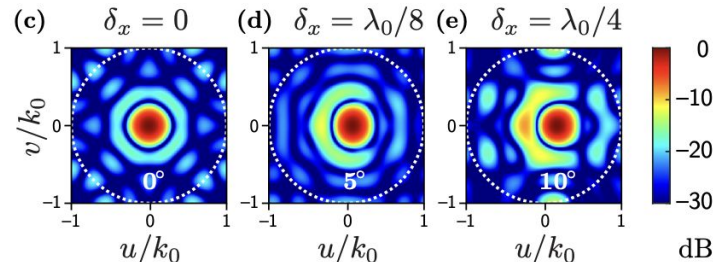
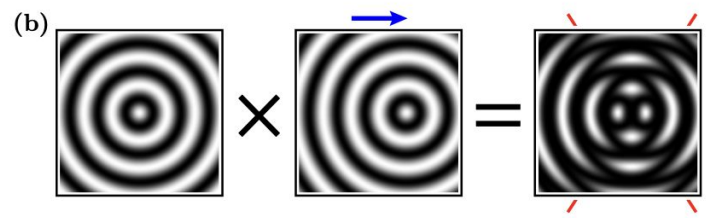
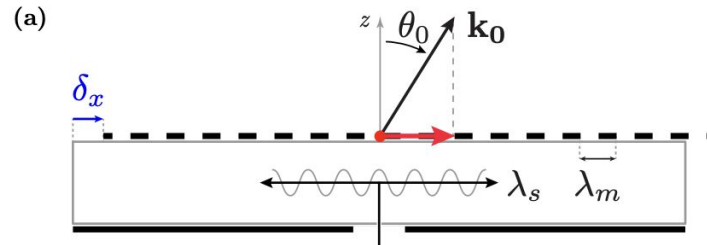
$$s_6(x, y) = s_0 e^{i \beta k_0^2 (x^2 + y^2)}, \quad m_6(x, y) = m_0 e^{-i \beta k_0^2 [(x - \delta_x)^2 + (y - \delta_y)^2]}.$$

Steering-law substitution

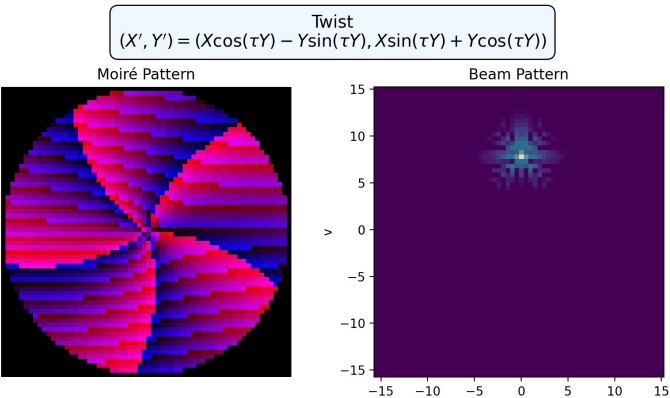
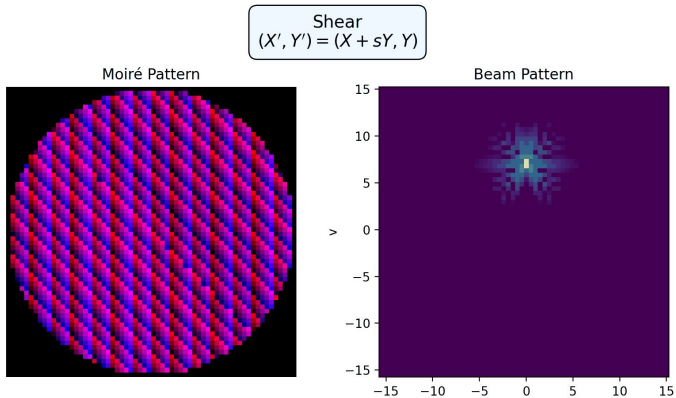
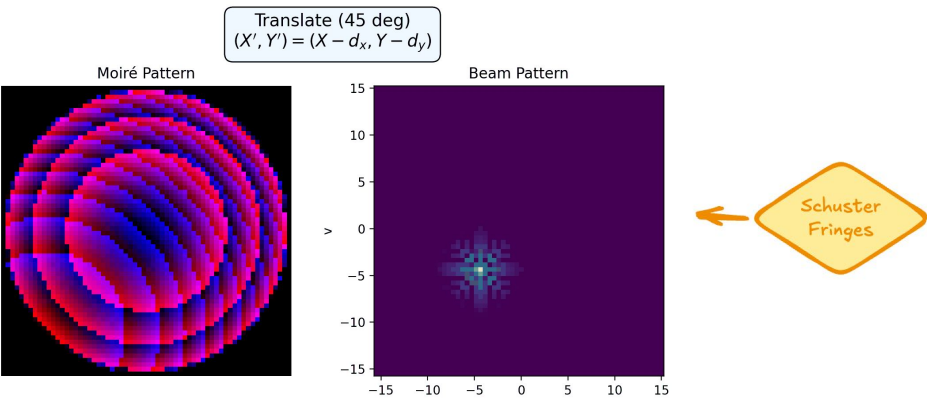
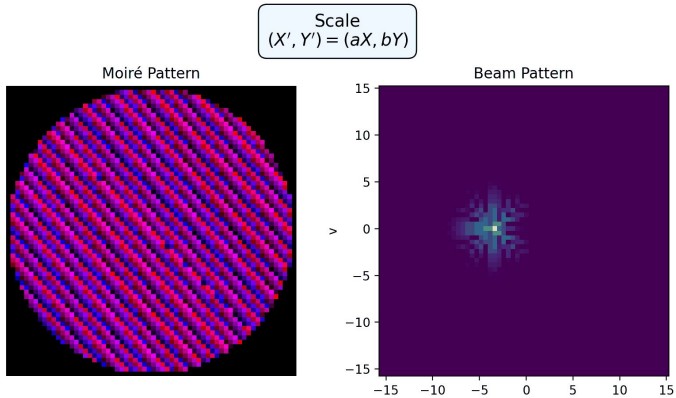
$$\begin{aligned} g_s(x, y) - g_m(T(x, y)) &= \beta k_0^2 [x^2 + y^2 - (x - \delta_x)^2 - (y - \delta_y)^2] \\ &= 2 \beta k_0^2 (\delta_x x + \delta_y y) - \beta k_0^2 (\delta_x^2 + \delta_y^2) = u_0 x + v_0 y + w_0, \end{aligned}$$

Translations are attractive vs. rotations in implementing, since no fast rotations around keyhole

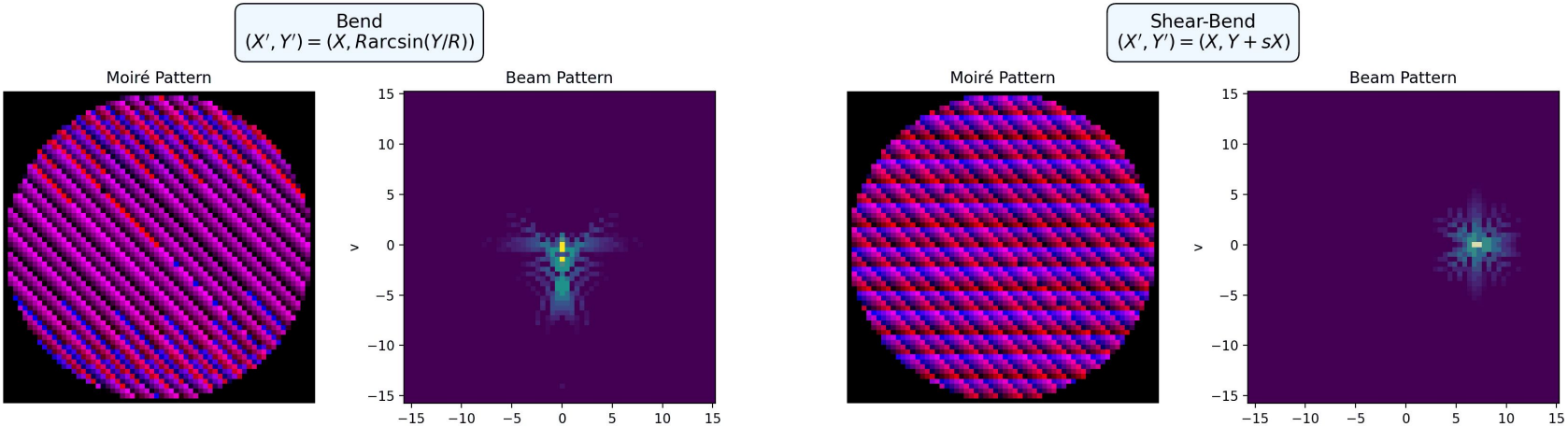
Circular Patterns for Fine Steering



Gallery



Non-Affine



A pure “bend” $T(x,y)=(x,f(y))$ is **non-affine**, but ...

How about Non-Analytical Patterns?

We can synthesize it numerically

How about control source-plane instead? electronically (like-ESA)

A dynamic source plane parameterized by a small set of electronic phase-shifter controls $\boldsymbol{\theta} = \{\theta_1, \dots, \theta_N\}$, find the optimal g_m

$$\min_{\boldsymbol{\theta}, g_m} \iint_{x,y} \left| g_s(x, y; \boldsymbol{\theta}) - g_m(T(x, y)) - (u_0 x + v_0 y + w_0) \right|^2 dx dy + \lambda \mathcal{R}[g_m].$$

Key Takeaways

Formulated a generalized mechanical-steering principle, deriving a novel beam-steering law.

Explored alternative mechanical steering techniques—such as Schuster-fringes translation—for simpler practical implementation.

Developed and validated a low-cost MSA design by integrating element-level phase control into the mask layer.

Demonstrated an E-band feeder-link system, showcasing its capacity and potential for next-generation satellite backhaul.

Thank you for your attention!

If you have any questions or comments, please feel free to contact
qitang2023@gmail.com

<https://github.com/dako2/moire-phased-array>

More Pics

